



**HAL**  
open science

## Auto-coherent homogenization applied to the assessment of thermal conductivity: Case of sugar cane bagasse fibers and moisture content effect

Cristel Onesippe Potiron, Ketty Bilba, Atika Zaknounge, Marie-Ange Arsène

### ► To cite this version:

Cristel Onesippe Potiron, Ketty Bilba, Atika Zaknounge, Marie-Ange Arsène. Auto-coherent homogenization applied to the assessment of thermal conductivity: Case of sugar cane bagasse fibers and moisture content effect. *Journal of Building Engineering*, 2021, 33, pp.101537. 10.1016/j.jobbe.2020.101537 . hal-03228172

**HAL Id: hal-03228172**

**<https://hal.univ-antilles.fr/hal-03228172>**

Submitted on 22 Aug 2022

**HAL** is a multi-disciplinary open access archive for the deposit and dissemination of scientific research documents, whether they are published or not. The documents may come from teaching and research institutions in France or abroad, or from public or private research centers.

L'archive ouverte pluridisciplinaire **HAL**, est destinée au dépôt et à la diffusion de documents scientifiques de niveau recherche, publiés ou non, émanant des établissements d'enseignement et de recherche français ou étrangers, des laboratoires publics ou privés.



Distributed under a Creative Commons Attribution - NonCommercial 4.0 International License

1 *Auto-coherent homogenization applied to the assessment of thermal conductivity: case of sugar cane*  
2 *bagasse fibers and moisture content effect*

3  
4 Cristel Onésippe Potiron<sup>1\*</sup>, Ketty Bilba<sup>1</sup>, Atika Zaknounge<sup>1</sup> and Marie-Ange Arsène<sup>1</sup>

5  
6 <sup>1</sup> Université des antilles - Laboratoire COVACHIM-M2E EA 3592, UFR SEN, Campus de  
7 Fouillole. BP 250 97157 Pointe-à-Pitre, Guadeloupe, France (FWI).

8  
9 \*corresponding author : [cristel.onesippe@univ-antilles.fr](mailto:cristel.onesippe@univ-antilles.fr)

10  
11 [ketty.bilba@univ-antilles.fr](mailto:ketty.bilba@univ-antilles.fr), [atika.zaknounge@univ-antilles.fr](mailto:atika.zaknounge@univ-antilles.fr), [marie-ange.arsene@univ-antilles.fr](mailto:marie-ange.arsene@univ-antilles.fr)

12  
13  
14 \*Phone : +590 (590) 483217

15  
16 Abstract

17 **The purpose of this study is** to evaluate the thermal conductivity of sugar cane bagasse  
18 fibers **when they reinforce** vegetable fibers/cement composites using auto-coherent  
19 homogenization. The moisture content effect on the thermal conductivity of composites  
20 is also studied. When the fiber content increases, porosity increases **according to a linear**  
21 **rule** and bulk density and thermal conductivity of composites decrease. When the  
22 moisture content grows, the thermal conductivity of composites increases. **When**  
23 **applying auto-coherent homogenization**, in dry state, **results show** a gap of less than  
24 10% between experimental and modeled values **of composites thermal conductivity and**  
25 **a mean sugar cane bagasse fibers thermal conductivity of 0.110 W/m.K.** In wet state  
26 (56% RH), there is an **approximate** agreement of 1,4% between estimated and  
27 experimental values of thermal conductivity of composites up to 4 wt% of fibers  
28 content.

29  
30 Keywords : Natural fibers ; Thermal properties ; Cement composites ; Auto – coherent  
31 homogenization; Moisture content.

32  
33 1. Introduction

34  
35 Guadeloupe (French West Indies) is a Caribbean island with a tropical climate [1, 2]  
36 were various vegetable fibers, including agro – industrial wastes, are low-cost and/or  
37 abundantly available [3-4]. This **archipelago** has a high seismicity and is prone to violent  
38 hurricanes [5]. Therefore, the main construction material used **in the building sector** is  
39 conventional cement and its derivatives (concrete blocks, bricks, ...) [6-7].

40 French thermal and acoustic regulations advocate the use of 50% renewable power in  
41 energy consumption by 2020 [7]. One way to reduce the energy consumption, as  
42 consequence to increase the renewable energy ratio, is to use less air-conditioning in  
43 infrastructures [7]. To achieve this goal, the partial replacement of cement by vegetable  
44 fibers as reinforcement of cementitious matrix **is considered** [1, 3, 6, 7]. Indeed,  
45 vegetable fibers **are known to** have insulating properties that is to say a low thermal  
46 conductivity and appear to be a good alternative to synthetic fibers such as glass fibers  
47 or asbestos fibers, commonly used for building insulation [8-10]. As observed by  
48 Onésippe et al. in 2010 [3] and even now, few works have demonstrated the low thermal  
49 conductivity of vegetable fibers cement-based composites as well as the thermal

50 conductivity of vegetable fibers (when they are incorporated in the composites) and the  
51 influence of moisture on thermal conductivity of these composites. The presence of  
52 wood fibers reduces the density of the material [11] and decreases its thermal  
53 conductivity [3, 6, 10].

54 Vegetable fibers are vulnerable to alkalinity of matrix thus causing debonding of the  
55 fiber / matrix interface and thus a decrease in the mechanical performance of the  
56 composites [3, 9]. To limit vulnerability of vegetable fibers in the matrix, various  
57 treatments of fibers have been considered such as chemical (acid or alkaline), physical-  
58 chemical, thermal and mechanical treatments [9, 11]. These various treatments lead to a  
59 strengthening of fiber/matrix interface [12] because they induce, on the one hand, the  
60 modification of the morphology of the fibers and, on the other hand, the reduction of the  
61 contents of hemicellulose and extractible materials which are inhibitors of the hydration  
62 of the binder [12].

63 Moreover, vegetable fibers are hydrophilic and their high affinity for water may thwart  
64 the hydration of matrix [13]. To overcome this competition, some authors propose the  
65 pyrolysis [12, 14] or the pre-wetting [15-18] of vegetable particles to retain their  
66 original volume (porosity) and so, play a role of water tank during the setting phase of  
67 the binder. Collet [13] recommends a pre-wetting of the binder with water prior to its  
68 addition to vegetable particles in order to ensure a good hydration of binder and to  
69 avoid competition between cement and fibers hydration [19].

70

71 The purposes of this study are to (1) estimate the modeled value of thermal conductivity  
72 of vegetable fibers when they reinforce cement matrix and (2) measure the effect of  
73 moisture content on vegetable fibers/cement composites thermal properties. To reach  
74 these goals, cement composites reinforced by various amounts of sugar cane bagasse  
75 fibers ranging from 2 to 8 wt % were considered. Sugar cane bagasse fibers are widely  
76 available in Guadeloupe : according to Food Directorate of Agriculture and Forestry  
77 from Guadeloupe, the island produces 680000 tons/year of sugar cane mainly used for  
78 the sugar and rum industries [20]. Bagasse is the solid lignocellulosic leftover after  
79 extraction of juice from the sugar cane stalk and is cheap compared to synthetic fibers  
80 [21].

81 In order to achieve the modeling of thermal conductivity of fibers, the first part is  
82 dedicated to the study of bagasse fibers / cement composites : measurements of thermal  
83 conductivity and physical-chemical characteristics (density, apparent volume and  
84 porosity). The thermal conductivity is studied at three different moisture contents. In  
85 the second part, a model of thermal conductivity of fibers and composites, in dry and  
86 wet states, is applied. The purposes of this work is (1) to propose a way to assess the  
87 thermal conductivity of bagasse fibers incorporated in this kind of composites, as very  
88 few data's of thermal conductivity of vegetable fibers are available and (2) to compare  
89 the (experimental and numerical) behaviors of composites when they are placed in  
90 different relative humidity (RH) to establish, if possible, a relation between thermal  
91 conductivity of composites and RH. Generally, in the literature, many models make it  
92 possible to estimate the thermal conductivity of dry concrete and dry composite  
93 materials on the basis of knowing the conductivity of each component and its  
94 concentration [22-27]. Several of them are based on the auto-coherent homogenization  
95 (HAC) model [25-28]. This model uses the statements of self-consistent field concept  
96 and of spherical geometry of inclusions in composites; for examples:

97 - autoclaved aerated concrete for Boutin [29],

- 98 - synthetic foams in continuous medium for Felske [30],
- 99 - wood shaving and concrete for Bederina et al. [25],
- 100 - cement composites containing rubber waste particles by Benazzouk et al.
- 101 [26],
- 102 - hemp concretes by Collet and Pretot [28] ,
- 103 - insulating building materials made from date palm fibers mesh by
- 104 Boukhattem et al. [26].

105 Among them, Felske [30], established equations allowing the estimation of the thermal  
106 conductivity of regular hollow spheres particles (synthetic foam), while the other  
107 previous authors [25-29] focused on a distribution of spherical particles with different  
108 diameter. Although the geometries involved are the same as in our materials, it appears  
109 that Felske's special case and critical values are not suitable in this study because Felske  
110 assumed that the particles are uniform. Bagasse fibers, being vegetable matter, are not  
111 uniform [31] and more, there is no perfect thermal contact between the vegetable  
112 matter and the cementitious matrix. Finally, the auto-coherent homogenization  
113 equations, as described by [25-29], were chosen because they are well suited to  
114 materials with very different pores sizes (such as concrete) [29] and they are currently  
115 employed when studying thermal conductivity of concrete.  
116 Thus, in this work on vegetable fibers/cement composite materials,

- 117 - a focus has been made on the model already confirmed and largely used in the
- 118 field of cementitious materials containing vegetable matter that is to say the
- 119 HAC model,
- 120 - this HAC model as described by [22-29] has been applied to assess the
- 121 numerical value of thermal conductivity of bagasse fibers/cement composites
- 122 in wet and dry states and it was possible for us to deduce the thermal
- 123 conductivity of sugar cane bagasse fibers in the cement composites.

124 To our knowledge, very few models of thermal conductivity of vegetable fibers / cement  
125 composites and even less models of the thermal conductivity of vegetable fibers alone  
126 are proposed in the literature [3, 8].

127

## 128 2. Materials

### 129 2.1 Sugar cane bagasse fibers

130 Sugar cane bagasse fibers are named NBF and were collected from Montebello distillery  
131 (Petit-Bourg, Guadeloupe, FWI). Fibers were crushed with a knife mill (Restch, France)  
132 and sieved in the laboratory to obtain final length varying from 1 to 10 mm and width  
133 between 0.4 and 1 mm. The sugar cane bagasse fibers chemical composition has already  
134 been determined [32] and is summarized in Table 1.

135

### 136 2.2 Binder

137 The binder was a white Portland cement CEM I 52.5 N manufactured by Axton society.  
138 This Portland cement CEM I 52.5N complies with European standard EN 197-1 [33]. Its  
139 chemical composition and some of its physical characteristics are presented in Table 2.

140

### 141 2.3 Composites formulations and preparation

142 A reference sample (i.e. without any fibers) has been prepared. It is named L.  
143 Composites were made by mixing each type of binder with various amounts of sugar  
144 cane bagasse fibers. Formulations of composites, named LFN, are presented in Table 3.  
145 All composites were prepared according to the mixing sequence indicated in Table 4 and  
146 tap water was used.  
147 The obtained pastes were casted in normalized molds of dimensions 40\*40\*160 mm<sup>3</sup>.  
148 According to EN 196-1 standard [34], a compaction (10 strokes by step – 2 steps) with a  
149 shaking table was applied to each sample. Then the isotropic samples, with a random  
150 repartition of fibers in the binder, were removed from the mold and left for curing  
151 during 28 days in a climatic chamber (25°C, RH = 70%).

### 152 153 3. Methods

#### 154 155 3.1 Bulk dry density, apparent volume and porosity measurements of composites

156 The bulk dry density  $\rho_A$  was deduced from the dry mass and apparent volume of  
157 samples. To determine the dry mass, samples were placed in an oven at 105°C (+/- 1°C).  
158 The dry state was reached once the mass of each sample was stabilized.  
159 The apparent volume of each sample was measured by using a sliding caliper (accuracy  
160 of +/- 0.01 mm). Each mean dimension is calculated from an average of three  
161 measurements.

162 Composites true density  $\rho_V$  has been measured using helium gas intrusion under helium  
163 gas flow with a “Pycnomatic” Thermo Electron Corporation equipment (France)  
164 pycnometer. Five measurements were conducted for each composite at 298 K, relative  
165 humidity of 70–80%. The open porosity  $\eta$  is deduced from bulk dry and true densities  
166 using equation (1):

$$167 \quad \eta = 1 - \frac{\rho_A}{\rho_V} \quad \text{equation 1}$$

168 where  $\rho_A$  is bulk dry density,  $\rho_V$  is true density of samples and  $\eta$  is open porosity.

#### 169 170 3.2 Thermal conductivity testing

171 The tests were performed with a C-therm TCi unit (Setaram, France). The C-Therm TCi  
172 employs the Modified Transient Plane Source (MTPS) technique. The one-sided,  
173 interfacial heat reflectance sensor applies a momentary constant heat source to the  
174 sample. A known current is applied to the sensor’s spiral heating element, providing a  
175 small amount of heat. The sensor’s guard ring is fired simultaneously supporting a one-  
176 dimensional heat exchange between the primary sensor coil and the sample. The  
177 current applied to the coil results in a rise in temperature at the interface between the  
178 sensor and sample, which induces a change in the voltage drop of the sensor element.  
179 The increase in temperature is monitored with the sensor’s voltage and is used to  
180 determine the thermo-physical properties of the sample. The thermal conductivity is  
181 inversely proportional to the rate of increase in the sensor voltage (or temperature  
182 increase). Thermal conductivity is measured directly [35].

183 For precise measurement of thermal conductivity, samples are first polished using a  
184 rotate polishing machine with sandpaper (Dremel, USA). Three levels of moisture are  
185 evaluated: 0%, 56% and saturated state 100% of relative humidity. We choose 56% RH  
186 as an intermediate value in relative humidity because, in real conditions, cement  
187 composites do not reach dry-oven or saturated conditions. The dry state (0% RH) is  
188 obtained by drying the material in an oven at 105°C (+/- 1°C) and then placing it in a

189 desiccator until the time of testing. To measure the thermal conductivity at 56 % RH,  
190 samples are placed in a desiccator whose humidity is controlled using saturated saline  
191 solutions of sodium bicarbonate. Local measurements are made on the lateral and  
192 transverse sides of samples and an average value is calculated. To ensure that the  
193 moisture content has not changed, samples are weighed before and after measurement.

194

### 195 3.3 Modeling of thermal conductivity of composites by auto-coherent homogenization

196 The auto-coherent homogenization is used in order to model the thermal conductivity of  
197 bagasse fibers / cement composites. This method was initially developed for the  
198 mechanical characterization of composites materials [25-26] and was then extended to  
199 electrostatic, magnetostatic, electric conduction and thermal properties, which are  
200 mathematically analogous [18, 28]. The principle of the method is that the  
201 heterogeneous material is assimilated to an equivalent homogeneous material, which  
202 must be characterized (knowledge of the conductivity of each component and its  
203 concentration). Thus, a transition of micro-scale (components) to macroscopic scale  
204 (material) allows to express overall thermal conductivity in terms of characteristics of  
205 each component (conductivity, volume concentration).

206

#### 207 3.3.1 Dry state

208 The auto-coherent homogenization is well described by Collet and Pretot [28]. Briefly,  
209 the dried material is considered as an assembly of spherical inclusions of various sizes.  
210 In the case of material with two-components, it is meant to be a sphere of radius  $R_a$  and  
211 thermal conductivity  $\lambda_a$  (component "a" is the air contained within the vegetable fibers)  
212 surrounded by a concentric shell of component "s" (s is the fiber block) of thermal  
213 conductivity  $\lambda_s$  and radius  $R_s$ .  $\lambda_d$  is the thermal conductivity of the equivalent  
214 homogeneous material also called effective conductivity (Figure 1).

215 The expression of effective conductivity  $\lambda_d$  (equation 2) is obtained by assuming that the  
216 energy contained in the heterogeneous medium is equivalent to that of the  
217 homogeneous medium under the same boundary conditions [26, 28].

218

$$219 \quad \lambda_d = \lambda_s = \left[ 1 + \frac{\varepsilon}{\frac{1-\varepsilon}{3} + \frac{1}{\lambda_a/\lambda_s - 1}} \right]; \quad \varepsilon = \left( \frac{R_a}{R_s} \right)^3 \quad \text{equation 2}$$

220

221 where  $\varepsilon$  is the volume concentration of air phase: it is assumed that the concentration of

unconnected phase is equal to the ratio of external and internal pores [29].

222 According to Boutin [29], this assumption is only satisfied if the material consists of an  
223 assembly of composites spheres of variable sizes. Collet and Pretot [28] made this same  
224 assumption in case of hemp concrete composites, which are close to bagasse  
225 cementitious composites of this study.

226

227 We assume that the fibers / dry binder composite is a three components material. In  
 228 that case, the tri-composite inclusion method is used for the modeling of thermal  
 229 conductivity assuming that a spherical air bubble “a” is surrounded by a concentric  
 230 vegetable particles shell “f” itself surrounded by a binder shell “s” (Figure 2).

231 This type of wildcard inclusion is based on three assumptions:

- 232 - the binder consists of cement and microscopic air bubbles trapped in closed-  
 233 pores;
- 234 - the vegetable particles consist of plant part and intra-particle air;
- 235 - the air bubble is the microscopic and macroscopic air contained in open pores of  
 236 material.

237 The expression of thermal conductivity of vegetable fibers / cement composites is  
 238 therefore given by equation 3.

239

$$\lambda = \lambda_s \left[ 1 + \frac{\theta}{1 + \frac{\delta \left( \frac{\lambda_a - 1}{\lambda_f} \right)}{3}} + \frac{1 - \theta}{3} + \frac{\frac{\lambda_a - 1}{\lambda_s} - \frac{\delta \left( \frac{\lambda_a - 1}{\lambda_f} \right) \left( \frac{2 \lambda_f}{\lambda_s} + 1 \right)}{3} \right]$$

equation 3

240

241 where  $\theta = 1 - \frac{1}{k+1} \left( \frac{\rho}{\rho_s} \right)$ ,  $\delta = \frac{\rho}{\rho_f} \frac{k}{k+1} \frac{1}{1 - \frac{\rho}{\rho_s} \frac{1}{k+1}}$  and  $k = m_f / m_s$

242  $\theta$  and  $\delta$  are concentrations directly calculated from the mass m of each component (of  
 243 known density  $\rho$ ). This definition of k is based on the assumption that the change of  
 244 properties between powdered cement and dry hydrated cement (i.e. hydrated cement at  
 245 0%RH) does not cause a significant variation in the thermal conductivity of composite  
 246 [15]. For each formulation, the characteristic parameter k is calculated as the ratio  
 247 between the mass of bagasse fibers and the mass of powdered cement [25].

248

### 249 3.3.2 Wet state

250 The modeling process of wet composite involves two steps:

- 251 - the first step allows creating homogeneous medium “sf” of vegetable particles “f”  
 252 and hydrated binder “s” at 0% RH,
- 253 - in the second step, the homogeneous medium “sf” is included in a tri-composite  
 254 (air, water, “sf”) model to obtain the final homogenized wet composite. The  
 255 vegetable fibers “f” and dry binder “s” are therefore considered as a  
 256 homogeneous medium “sf” and not as two separated phases (Figure 3).

257 Equation 4 gives the expression of equivalent conductivity of “sf” composite as a  
 258 function of conductivity of each component (fibers and hydrated binder at 0% RH). The  
 259 parameter  $\varepsilon'$  is used to evaluate the volume concentration of fibers in the binder.

$$\lambda_{sf} = \lambda_s \left[ 1 + \frac{\varepsilon'}{\frac{1-\varepsilon'}{3} + \frac{1}{\lambda_f/\lambda_s - 1}} \right] ; \quad \varepsilon' = \left( R_f / R_s \right)^3 = \frac{1}{1 + k \frac{\rho_f}{\rho_s}} \quad \text{equation 4}$$

261 where  $\lambda$  is for the thermal conductivity,  $k$  is the ratio of mass (as defined in equation 3)  
 262 and  $\rho$  is the density.

263 In the second step, the tri-composite inclusions model allows expressing the  
 264 conductivity of composite in wet states (equation 5).

$$\lambda_H = \lambda_{sf} \left[ 1 + \frac{\theta}{\frac{1-\theta}{3} + \frac{1 + \frac{\delta}{3} \left( \frac{\lambda_a}{\lambda_w} - 1 \right)}{\frac{\lambda_a}{\lambda_w} - 1 - \frac{\delta}{3} \left( \frac{\lambda_a}{\lambda_w} - 1 \right) \left( 2 \frac{\lambda_w}{\lambda_{sf}} + 1 \right)}} \right] \quad \text{equation 5}$$

$$k_1 = \frac{m_w}{m_s + m_f}, \quad \theta = \left( \frac{R_w}{R_{sf}} \right)^3 = 1 - \frac{1}{1 + k_1} \frac{\rho_h}{\rho_{sf}} \quad \text{and} \quad \delta = k_1 \frac{\rho_{sf}}{\rho_w} \left( \frac{1}{1 - \frac{\rho_H}{\rho_{sf}} \frac{1}{k_1 + 1}} - 1 \right)$$

267  $\lambda$  is for the thermal conductivity,  $k$  is the ratio of mass of water (w) related mass of  
 268 cement (s) + mass of fibers (f).

269  $\theta$  and  $\delta$  are concentrations directly calculated from the mass  $m$  of each component (of  
 270 known density  $\rho$ )

271

#### 272 4. Results and discussion

273 In order to estimate thermal conductivity of vegetable fibers, some properties of  
 274 composites are required: physical properties (bulk dry density, open porosity) and  
 275 thermal conductivity.

276

##### 277 4.1 Bulk density and open porosity of composites at 0% RH

278 Figure 4 reports the variation of bulk density as a function of the fiber contents for LFN  
 279 composites in the dry state. As expected, the more the fiber content, the lower the bulk  
 280 density is [36]. The first significant decrease is obvious: it corresponds to the addition of  
 281 2% by weight of bagasse fibers, which are a lightweight material. Between 2 and 4% by  
 282 weight of fibers, there is a light decrease. After 4 wt%, bulk density decreased at a  
 283 relatively constant rate with increased fiber content as observed by [37].

284 Figure 5 presents the evolution of LFN composites porosity according to their fiber  
 285 content in the dry state.

286 Porosity of material is gradually increasing with the amount of bagasse fibers. This  
 287 increase with addition of fibers is explained by the formation of air voids in the  
 288 microstructure of paste (due to the presence of fibers which are porous) and the voids  
 289 content becomes high as fiber volume fraction increases [36]. Moreover, short fibers, as  
 290 used in this study, are considered to be more difficult to align and pack densely. The

291 packing of short fibers in cement paste leads to increase the amount of voids [10] and  
292 therefore porosity.

293

## 294 4.2 Thermal conductivity of composites

### 295 4.2.1 Experimental thermal conductivity

#### 296 4.2.1.1 Dry state

297 Figure 6 illustrates the evolution of thermal conductivity of LFN composites according to  
298 fiber content at 0% of relative humidity. According to Demirboga [38], thermal  
299 conductivity of Portland cement type I is (1.230 +/- 0.050) W/m.K.

300 The purpose of including vegetable fibers in cement is to develop a more insulating  
301 material than cement in order to use it as an interior partition or an interior insulating  
302 coating in the housing, for examples. It would help to prohibit the leaking of heat on  
303 both sides of the partitions [36]. First, as expected, the thermal conductivity of Portland  
304 cement is strongly decreased (by a factor of around 2) by introducing 2 wt % of  
305 vegetable fibers. Then, thermal conductivity of cement samples decreases slightly when  
306 increasing fiber content [10, 27, 36]. This decrease follows a logarithmic evolution.  
307 According to [3], thermal conductivity of treated bagasse fibers is lower than that of  
308 cement paste, so we assume it's the same for raw bagasse fibers: its thermal  
309 conductivity is lower than that of cement. Consequently, this decrease is expected with  
310 law of mixture. Moreover, thermal conductivity is inversely proportional to the voids in  
311 composites [10, 39] and as shown by Figure 5, porosity of samples increases with the  
312 fiber content. Based on these results, the linear relation between the thermal  
313 conductivity  $k$  of bagasse composites and bulk density  $\rho$  is:

$$314 \quad k = 0.0005\rho - 0.0924 \quad (R^2 = 0.78267) \quad \text{equation 6}$$

315 where  $k$  is thermal conductivity and  $\rho$  bulk density.

316 Equation 6 is consistent with classical equations applied to evaluate thermal  
317 conductivity of insulating materials used in the field of construction [39].

318

#### 319 4.2.1.2 Sensitivity of thermal conductivity to moisture content

320 Thermal conductivity was also studied for the same composites at 56% and 100% of  
321 relative humidity (saturated state).

322 Fibrous media are known to often have a geometric anisotropy linked (1) to the  
323 anisotropy of the fibers themselves and (2) to their orientation within the material. In  
324 the case of vegetable fibers, an anisotropy of the thermal properties appears locally, as  
325 the tensor of conductivity of fibers is generally orthotropic [38]. We assume that the  
326 thermal conductivity of studied composites is isotropic because fibers are randomly  
327 oriented and properties of short fibers (in this study, length varying from 1 to 10 mm  
328 and width between 0.4 and 1 mm) composites are isotropic [41].

329 Figure 7 presents the thermal conductivity of samples according to their bulk density for  
330 different moisture contents.

331 The more the percentage of pores, the lighter the specimen are and the lower their  
332 thermal conductivities are as observed by others [10]. That is to say that the lighter a  
333 material is and the better is its insulating power. The thermal conductivity of the  
334 composites in saturated conditions is greater than in the dry state [27]. This fact is  
335 explained by the thermal conductivity of water, which is 25 times higher than air [42];

336 the presence of air will alter the overall thermal conductivity of the material by  
337 decreasing it. The composite subjected to a relative humidity of 56% exhibited a mass  
338 gain of 4 to 8% (in comparison with dry state), which involves the increase from 15 to  
339 50% of the thermal conductivity of materials. For moisture contents close to saturation,  
340 the thermal conductivity of the composite increases by around 100 % of its value in the  
341 dry state. These results are in accordance with those exhibited by Asadi et al. [39].

342

## 343 4.2.2 Numerical thermal conductivity

### 344 4.2.2.1 Dry state

345 Firstly, by knowing the thermal conductivity of pure hardened cement paste,  $\lambda_d$  and its  
346 porosity measured with helium pycnometer, we can calculate the conductivity of solid  
347 particles  $\lambda_s$  using equation 2. The value of  $\lambda_s$  is 1.125 W/m.K.

348 To estimate thermal conductivity of fibers, the auto-coherent method applied to three  
349 phases medium (equation 3) is used in combination with least squares method of  
350 minimization. The mean square deviation between experimental and numerical thermal  
351 conductivities of dry composites is minimized and bagasse fibers thermal conductivity is  
352 estimated. Its average value is about 0.110 W/m.K. This value is consistent with the  
353 values estimated by Onésippe et al. [3] for treated bagasse fibers.

354 Figure 8 shows that the theoretical values calculated using equation 3 are consistent  
355 with the experimental measurements in the case of dry composites, whatever the bulk  
356 density. A gap of less than 10% is obtained.

357

### 358 4.2.2.2. Wet state (100% RH)

359 As with the previous model, a comparison of the results is made in the case of wet  
360 composites (56% RH, Figure 9 and 100% RH, Figure 10). For 56% RH, there is a good  
361 agreement between numerical and experimental values in low fibers contents (approx.  
362 less than 4 wt%), which correspond to bulk densities greater than 1360 kg/m<sup>3</sup>. Below  
363 this value, it seems that the model underestimates thermal conductivity of composites  
364 by about 10 to 20%. This underestimation reaches nearly 30% at saturated state (100%  
365 RH), whatever the bulk density, as shown by Figure 10. The model used for numerical  
366 calculation considered the shape of the aggregates to be spherical. This underestimation  
367 may be due to the geometrical distribution of void phase that is to say distribution of  
368 pore structure. This difference can also be explained by conduction phenomenon due to  
369 free water or entrapped water that implies the use of a more complex modeling to  
370 explain the behavior. Moreover, the experimental conductivity is the average of local  
371 measurements that depend on surface conditions, orientation of fibers and compacting  
372 direction. In addition, polishing of samples with high fiber content is difficult and can  
373 cause local differences in thickness.

374 The thermal conductivity calculated by the model seems to be little sensitive to changes  
375 induced by the generic water cell. This little sensitivity is explained by low volume of  
376 water adsorbed in this range of humidity.

377

## 378 5. Perspectives

379 Generally, in Guadeloupe, the relative humidity of the air varies between 70% and 80%  
380 [42], that is to say that the thermal conductivity of composites would be greater than in  
381 the dry state. The composites of this study cannot be considered as insulating materials  
382 for our climatic conditions. In order to decrease their thermal conductivity, we

383 considered treatment of bagasse fibers before incorporating them into Portland cement.  
384 We choose to analyze the effect of pyrolysis treatment on sorption/desorption  
385 behaviors of the bagasse fibers. The sorption isotherm of natural bagasse fibers NBF is  
386 compared to that of pyrolyzed fibers, TBF which are prepared under controlled inert  
387 atmosphere (N<sub>2</sub> flow, 2 L/h) during 2 h at 240°C [43]. It is obtained experimentally by  
388 assessing the moisture content of the product in equilibrium with different air relative  
389 humidity at an average temperature of (22±3) °C. Relative humidity is controlled by  
390 saturated saline solutions according to ISO-12571 norm [44]. The moisture content  $w$  is  
391 deduced using the equation 7:

392 
$$w = \frac{m - m_0}{m_0} \quad \text{equation 7}$$

393 Where  $m$  and  $m_0$  are the mass of the sample in respectively steady state conditions and  
394 initial dry state.

395 In Figure 11, the isotherms present a S-shape corresponding to the type IV of the Rogers  
396 classification. This behavior is frequently observed in cellulose-based materials [45]. We  
397 can see that pyrolyzed bagasse fibers are less hygroscopic than natural bagasse fibers,  
398 particularly at high relative humidity (decrease of 30% of its sorption capacity). Indeed,  
399 hemicellulose degradation during pyrolysis (between 160 and 260°C) [32] makes the  
400 TBF less sensitive to moisture; generally, they become more hydrophobic [3]. This last  
401 point encourages us to develop pyrolyzed bagasse fiber / cement composites. As  
402 mentioned by Collet and Pretot [28], thermal conductivity of hygroscopic materials  
403 increases with moisture content. The pyrolyzed fibers being more hydrophobic [3] than  
404 the raw fibers, they would generate less moisture in the composites that is to say that  
405 the ratio air/water will be increased. As thermal conductivity of air is lower than that of  
406 water [35], the resulting composites would have lower thermal conductivities (if we  
407 consider a simple law of mixture) than the LFN and would allow our materials to be  
408 considered as insulating materials in the field of construction.

409

## 410 6. Conclusions

411 A theoretical modeling based on auto-coherent homogenization is proposed to estimate  
412 the thermal conductivity of bagasse fibers, that is a novelty. The model is also used to  
413 estimate the conductivity of fibers and cement and then the conductivity of composites  
414 under both dry (good fitting with the model) and wet conditions.

415 The bagasse fibers / cement composites materials present low thermal conductivity.  
416 The study shows that the thermal conductivity of such composites depends both on  
417 fibers / cement ratio (bulk density) and moisture content. The best insulating properties  
418 are obtained with an untreated bagasse fiber content around 8 % wt.

419 Further investigations on pores size and distribution are required in order to improve  
420 the accuracy of the model in wet conditions.

421 We explore the isotherm sorption of pyrolyzed bagasse fibers. These data confirm that  
422 the pyrolysis allows obtaining more hydrophobic fibers, which once included in cement,  
423 would provide more insulating materials for building applications.

424

## 425 Acknowledgements

426 We thank for the financial support (1) the Région Guadeloupe and european funds for  
427 projects "Développement d'isolants thermiques à partir de fibres végétales : ISOCFV"  
428 (n°32524) and (2) the Agence Nationale de la Recherche for the project

429 "AWaPUMat/Résidus industriels, leurs usages potentiels comme matériaux pour  
430 l'habitation et la construction" (n° ANR-12-IS09-0002-01).

431  
432  
433

## 434 **References**

435

436 [1] M.A. Arsène, K. Bilba, C. Onésippe, L. Rodier, Thermal and flexural properties of  
437 bagasse/cement composites, *J. Green Mater.* (2016).  
438 <http://dx.doi.org/10.1680/jgrma.1500012>

439 [2] R.C. Dromard, Y. Bouchon-Navaro, S. Cordonnier, C. Bouchon, The invasive lionfish,  
440 *Pterois volitans*, used as a sentinel species to assess the organochlorine pollution by  
441 chlordecone in Guadeloupe (Lesser Antilles), *J. Mar. Pol. Bul.* 107 (2016) 102-106.  
442 <https://doi.org/10.1016/j.marpolbul.2016.04.012>

443 [3] C. Onésippe, N. Passé-Coutrin, F. Toro, S. Delvasto, K. Bilba, M.A. Arsène, Sugar cane  
444 bagasse fibres reinforced cement composites : Thermal considerations, *J. Compos. Part A*  
445 *Appl. Sci. Manuf.* 41 (2010) 549-556.  
446 <https://doi.org/10.1016/j.compositesa.2010.01.002>

447 [4] J. Faverial, J. Sierra, Home composting of household biodegradable wastes under the  
448 tropical conditions of Guadeloupe (French Antilles), *J. Cleaner Prod.* 83 (2014) 238-244.  
449 <https://doi.org/10.1016/j.clepro.2014.07.068>

450 [5] N. Zahibo, E. Pelinovsky, T. Talipova, A. Rabinovich, A. Kurkin, I. Nikolchina, Statistical  
451 analysis of cyclone hazard for Guadeloupe, Lesser Antilles, *Atmosph. Res.* 84 (2007) 13-  
452 29. <https://doi.org/10.1016/j.atmosres.2006.03.008>

453 [6] L. Rodier, Matériaux de construction en zone tropicale humide - Potentialités de sous  
454 produits ou de matériaux naturels locaux en substitution ou en addition à la matrice  
455 cimentaire, Doctoral thesis (2014), Université des Antilles et de la Guyane (France)

456 [7] L. Rodier, K. Bilba, C. Onésippe, M.A. Arsène, Utilization of bio-chars from sugarcane  
457 bagasse pyrolysis in cement-based composites, *J. Ind. Crop* 41 (2019) 111731.  
458 <https://doi.org/10.1016/j.indcrop.2019.111731>

459 [8] J.C. Damfeu, P. Meukam, Y. Jannot, Modeling and measuring of the thermal properties  
460 of insulating vegetable fibers by the asymmetrical hot plate method and the radial flux  
461 method : Kapok, coconut, groundnut shell fiber and rattan, *J. Thermochimica Acta* 630  
462 (2016) 64-77. <https://doi.org/10.1016/j.tca.2016.02.007>

463 [9] V. Agopyan, H. Savastano Jr., V. M. John, M. A. Cincotto, Developments on vegetable  
464 fibre-cement based materials in Sao Paulo, Brazil : an overview, *J. Cem. Concr. Compos.*  
465 27 (2005) 527-536. <https://doi.org/10.1016/j.cemconcomp.2004.09.004>

466 [10] J. Khedari, B. Suttisonk, N. Prathinthong, J. Hirunlabh, New lightweight composite  
467 construction materials with low thermal conductivity, *J. Cem. Concr. Comp.* 23 (2001)  
468 65-70. [https://doi.org/S0958-9465\(00\)00072-X](https://doi.org/S0958-9465(00)00072-X).

469 [11] V. Da Costa Correia, S.F. Santos, H. Savastano Junior, Vegetable fiber as reinforcing  
470 elements for cement based composite in housing applications – a Brazilian experience,  
471 *MATEC Web Conf.* 149 (2018) 01007.  
472 <https://doi.org/10.1051/mateconf/201814001007>

473 [12] M.-A. Arsène, K. Bilba, C. Onésippe, 4- Treatments to viable utilization of vegetable  
474 fibers in inorganic-based composites, in : H. Savastano Junior, J. Fiorelli, S. F. dos Santos  
475 (Eds.), Sustainable and nonconventional construction materials using inorganic bonded  
476 fiber composites, Woodhead publishing Inc., Sao Paulo, 2017, pp. 69-123

477 [13] F. Collet, Caractérisations hydrique et thermique de matériaux de génie civil à  
478 faibles impacts environnementaux, Doctoral thesis (2004), INSA de Rennes (France)

479 [14] S.F. Santos, G.H.D. Tonoli, J.E.B. Mejia, J. Fiorelli, H. Savastano Junior, Non-  
480 conventional cement-based composites, reinforced with vegetable fibers: A review of  
481 strategies to improve durability, *Materiales de Construcción* 65 (2015) e041.  
482 <https://doi.org/10.3989/mc.2015.05514>.

483 [15] V. Cerezo, Propriétés mécaniques, thermiques et acoustiques d'un matériau à base  
484 de particules végétales, Doctoral thesis (2005), INSA de Rennes (France)

485 [16] P. Coatanlem, R. Jauberthie, F. Rendell, Lightweight wood chipping concrete  
486 durability, *J. Constr. Build. Mater.* 20 (2006) 776-781.  
487 <https://doi.org/10.1016/j.conbuildmat.2005.01.057>

488 [17] T.T. Nguyen, V. Picandet, S. Amziane, C. Baley, Influence of compactness and hemp  
489 hurd characteristics on the mechanical properties of lime and hemp concrete, *European*  
490 *journal of environmental and civil engineering* 13 (2009) 1039-1050. [https://doi.org/](https://doi.org/10.3166/regc.13.1039-1050)  
491 [10.3166/regc.13.1039-1050](https://doi.org/10.3166/regc.13.1039-1050)

492 [18] P. Monreal, L.B. Mboumba-Mamboundou, R.M. Dheilly, M. Queneudec, Effects of  
493 aggregate coating on the hygral properties of lignocellulosic composites, *J. Cem. Concr.*  
494 *Compos.* 33 (2011) 301-308. <https://doi.org/10.1016/j.cemconcomp.2010.10.017>

495 [19] J. Page, F. Khadraoui, M. Gomina, M. Boutouil, Influence of different surface  
496 treatments on the water absorption of flax fibres : rheology of fresh reinforced-mortars  
497 and mechanical properties in the hardened state, *Constr. Build. Mater.* 199 (2019) 424-  
498 434. <https://doi.org/10.1016/j.conbuildmat.2018.12.042>

499 [20] Direction de l'Alimentation, de l'Agriculture et de la Forêt de Guadeloupe.  
500 <http://daaf.guadeloupe.agriculture.gouv.fr/Canne-a-sucre>, 2019 (accessed 09 april  
501 2019)

502 [21] S.G. Karp, A. Lorenci Woiciechowski, V.T. Soccol, C. R. Soccol, Pretreatment  
503 strategies for delignification of sugarcane bagasse: a Review, *Braz. Arch. Biol. Technol.*  
504 *56* (2013) 679-689.

505 [22] M.I. Khan, Factors affecting the thermal properties of concrete and applicability of  
506 its prediction models, *J. Build. and Environ.* 37 (6) (2002) 607-614.  
507 [https://doi.org/10.1016/S0360-1323\(01\)00061-0](https://doi.org/10.1016/S0360-1323(01)00061-0)

508 [23] J. Wang, J.K. Carson, M.F. North, D.J. Cleland, A new structural model of effective  
509 thermal conductivity for heterogeneous materiald with co-continuous phases,  
510 *International J. Heat Mass Transfer* 21 (9-10) (2008) 2389-2397.  
511 <https://doi.org/10.1016/j.ijheatmasstransfer.2007.08.028>

512 [24] P.K. Samantray, P. Karthikeyan, K.S. Reddy, Estimating effective thermal  
513 conductivity of two-phase materials, *J. Heat Mass Transfer* 49 (21-22) (2006) 4209-  
514 4219. <https://doi.org/10.1016/j.ijheatmasstransfer.2006.03.015>

515 [25] M. Bederina, L. Marmoret, K. Mezreb, M.M. Khenfer, A. Bali, M. Quéneudec, Effect of  
516 addition of wood shavings on the thermal conductivity of sand concretes : experimental  
517 study and modelling, *J. Constr. Build. Mater.* 21 (2007) 662-668.  
518 <https://doi.org/10.1016/j.conbuildmat.2005.12.008>

519 [26] A. Benazzouk, O. Douzane, K. Mezreb, B. Laidoudi, M. Quéneudec, Thermal  
520 conductivity of cement composites containing rubber waste particles : experimental  
521 study and modelling, *J. Constr. Build. Mater.* 22 (2008) 573-579.  
522 <https://doi.org/10.1016/j.conbuildmat.2006.11.011>

523 [27] L. Boukhattem, M. Boumhaout, H. Hamdi, B. Benhamou, F. Ait Nouh, Moisture  
524 content influence on the thermal conductivity of insulating building materials made

525 from date palm fibers mesh, *J. Constr. Build. Mater.* 148 (2017) 811-823.  
526 <https://doi.org/10.1016/j.conbuildmat.2017.05.020>

527 [28] F. Collet, S. Pretot, Thermal conductivity of hemp concretes: Variation with  
528 formulation, density and water content, *J. Constr. Build. Mater.* 65 (2014) 612-619  
529 <https://doi.org/10.1016/j.conbuildmat.2014.05.039>

530 [29] C. Boutin, Thermal conductivity of autoclaved aerated concrete: modeling by the  
531 self-consistent method, *J. Mater. Struct.* 29 (1996) 609-615  
532 <https://doi.org/10.1007/BF02485968>

533 [30] J.D. Felske, Effective thermal conductivity of composite spheres in a continuous  
534 medium with contact resistance, *Int. J. Heat Mass Transf.* 47 (2004) 3453-3461  
535 <https://doi.org/j.ijheatmasstransfer.2004.01.013>

536 [31] G. Ruano, F. Bellomo, G. Lopez, A. Bertuzzi, L. Nalim, S. Oller, Mechanical behavior of  
537 cementitious composites reinforced with bagasse and hemp fibers, *J. Construct. Build.*  
538 *Mater.* 240 (2020) 117856  
539 <https://doi.org/10.1016/j.conbuildmat.2019.117856>

540 [32] K. Bilba, M.-A. Arsène, A. Ouensanga, Sugar cane bagasse reinforced cement  
541 composites. Part I. Influence of the botanical components of bagasse on the setting of  
542 bagasse/cement composite, *J. Cem. Concr. Compos.* 25 (2003) 91-96.  
543 [https://doi.org/10.1016/S0958-9465\(02\)00003-3](https://doi.org/10.1016/S0958-9465(02)00003-3)

544 [33] EN 197-1, Ciment – Partie 1 : composition, spécifications et critères de conformité  
545 des ciments courants, NF European Standards, 2001

546 [34] EN 196-1, Méthodes d'essais des ciments – Partie 1 : détermination des résistances  
547 mécaniques, NF European Standards, 2006

548 [35] SETARAM. [https://www.setaram.fr/wp-content/uploads/2016/01/C-Therm-TCi-](https://www.setaram.fr/wp-content/uploads/2016/01/C-Therm-TCi-Thermal-Conductivity-2016.pdf)  
549 [Thermal-Conductivity-2016.pdf](https://www.setaram.fr/wp-content/uploads/2016/01/C-Therm-TCi-Thermal-Conductivity-2016.pdf), 2019 (accessed 11 april 2019)

550 [36] A. Al-Ghaban, H.A. Jaber, A.A. Shaher, Investigation of addition different fibers on  
551 the performance of cement mortar, *J. Eng. Tech. Part A* 36 (2018) 957-965.  
552 <http://dx.doi.org/10.30684/etj.36.9A.3>

553 [37] H. Savastano Jr., P.G. Warden, R.S.P. Coutts, Brazilian waste fibres as reinforcement  
554 for cement-based composites, *J. Cem. Concr. Compos.* 22 (2000) 379-384.  
555 [https://doi.org/10.1016/S0958-9465\(00\)00034-2](https://doi.org/10.1016/S0958-9465(00)00034-2)

556 [38] R. Demirboga, Thermal conductivity and compressive strength of concrete  
557 incorporation with mineral admixtures, *J. Build. Env.* 42 (2007) 2467-2471.  
558 <http://dx.doi.org/10.1016/j.jbuidenv.2006.06.010>

559 [39] I. Asadi, P. Shafigh, Z. Fitri Abu Hassan, N. Bindi Mahyuddin, Thermal conductivity of  
560 concrete – a review, *J. Build. Eng.* 20 (2018) 81-93.  
561 <https://doi.org/10.1016/j.job.2018.07.002>

562 [40] R. El-Sawalhy, J. Lux, P. Salagnac, Caractérisation et prédiction des propriétés  
563 thermiques des laines de chanvre à l'aide d'images tomographiques, Conference paper  
564 (2013)

565 [41] Gaurav, H. Gohal, V. Kumar, H. Jena, Study of natural fibre composite and its  
566 hybridization techniques, *J. Mater. Today: Proceedings* (2020) *In press*  
567 <https://doi.org/10.1016/j.matpro.2020.02.277>

568 [42] Weather online, 2019 (accessed 11 april 2019)  
569 [https://www.wofrance.fr/weather/maps/city?WMO=78897&CONT=mamk&LAND=AT](https://www.wofrance.fr/weather/maps/city?WMO=78897&CONT=mamk&LAND=AT&ART=RLF&LEVEL=150)  
570 [&ART=RLF&LEVEL=150](https://www.wofrance.fr/weather/maps/city?WMO=78897&CONT=mamk&LAND=AT&ART=RLF&LEVEL=150)

571 [43] K. Bilba, M.-A. Arsène, Silane treatment of bagasse fiber for reinforcement of  
572 cementitious composites, *J. Compos. Part A Appl. Sci. Manuf.* 39 (2008) 1488-1495.  
573 <https://doi.org/10.1016/j.compositesa.2008.05.013>

574 [44] ISO-12571 Performance hygrothermique des matériaux et produits pour le  
575 bâtiment – Détermination des propriétés de sorption hygroscopiques, International  
576 Organization for Standardization, 2013  
577 [45] A. Bessadok, D. Langevin, F. Gouanvé, C. Chappéy S. Roudesli, S. Marais, Study of  
578 water sorption on modified agave fibres, Carbohydr. Polym. 76 (2009) 74-85.  
579 <https://doi.org/10.1016/j.carbpol.2008.09.033>

580

## 581 **Figures caption**

582

583 Figure 1: Auto-coherent method applied to two-phase medium - geometry of an  
584 elementary inclusion composite

585 Where  $R_a$  and thermal conductivity  $\lambda_a$  (component “a” is the air contained within the  
586 vegetable fibers) surrounded by a concentric shell of component “s” (s is the fiber block)  
587 of thermal conductivity  $\lambda_s$  and radius  $R_s$ ,  $\lambda_a$  is the thermal conductivity of the equivalent  
588 homogeneous material also called effective conductivity

589

590 Figure 2: Auto-coherent method applied to three-phase medium - geometry of an  
591 elementary inclusion composite

592 Where a spherical air bubble “a” is surrounded by a concentric vegetable particles shell  
593 “f” itself surrounded by a binder shell “s”

594

595 Figure 3 : Double homogenization of auto-coherent model (binder+ vegetable particles)  
596 Where a is for air, w is for water and H for hydrated composite

597

598 Figure 4 : Bulk density of composites according to their fiber content in the dry state  
599 (RH = 0%)

600

601 Figure 5 : Porosity of composites according to their fiber content in the dry state (RH =  
602 0%)

603

604 Figure 6 : Experimental thermal conductivity of LFN composites according to their fiber  
605 content in the dry state (RH = 0%)

606

607 Figure 7 : Experimental thermal conductivity of LFN composites according to their bulk  
608 density at different moisture contents

609

610 Figure 8 : Comparison between numerical calculations and experimental results of  
611 composites thermal conductivity in the dry state according to bulk density

612

613 Figure 9 : Thermal conductivity varying with bulk density: comparison between  
614 numerical calculations and experimental results in the wet state (RH=56%)

615

616 Figure 10: Thermal conductivity varying with bulk density: comparison between  
617 numerical calculations and experimental results in the wet state (RH=100%)

618

619 Figure 11 : Isotherm sorption of natural (NBF) and pyrolyzed bagasse fibers (TBF) at  
620 (22±3)°C. In red: sorption; in green: desorption.

621

622

623 Table 1: Botanical composition of raw sugar cane bagasse fibers (NBF) [29].

624

Cellulose	Hemicellulose	Lignin	Extractives	Humidity	Sum (except humidity)
wt %	wt %	wt %	wt %	wt %	wt %
48.68	25.46	21.94	3.92	7.50	100

625

626

627 Table 2: Chemical composition and some physical characteristics of CEM I 52,5 N [5].

628

Content wt %						
SiO <sub>2</sub>	Fe <sub>2</sub> O <sub>3</sub>	Al <sub>2</sub> O <sub>3</sub>	CaO	Na <sub>2</sub> O	K <sub>2</sub> O	MgO
21.45	0.22	4.08	65.05	0.06	0.20	0.49
Loss on ignition (wt %)						
1.45						
Bulk density (g/cm <sup>3</sup> )						
3.08						
Median particle size (µm)						
15.70						
Specific area (cm <sup>2</sup> /g)						
4200						

629

630

631 Table 3 : Formulations of LFN composites.

632

Composites	Binder	NBF/binder ratio (by mass)	Water/binder ratio (by mass)	Mass (g) relative to 1000 g of cement paste		
				NBF	CEM I	Water
L (without fibers)	1	0	0.4	0	704	296
LFN1	1	0.02	0.60	12.3	617.3	370.4
LFN2	1	0.03	0.60	18.4	613.5	368.1
LFN3	1	0.04	0.60	24.4	609.8	365.8
LFN4	1	0.05	0.60	30.3	606.1	363.6
LFN5	1	0.08	0.60	47.6	595.2	357.2

633

634

635 Table 4 : Mixing sequence of elaboration of composites.

636

Mixing sequence	Time
Adding the pre-wetted binder in the mixing container	0
Mixing the binder at slow speed (140 rpm)	30 s
Adding the rest of the water	30 s
Mixing at high speed (285 rpm)	2 min
Progressive addition of vegetable fibers	2 min
Mixing at high speed (285 rpm)	5 min

637

Figure 1 : Auto-coherent method applied to two-phase medium - geometry of an elementary inclusion composite

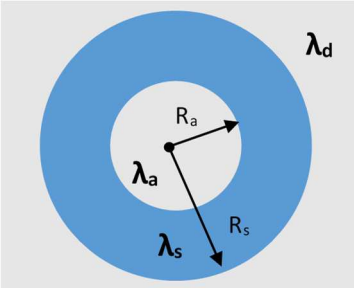


Figure 2 : Auto-coherent method applied to three-phase medium - geometry of an elementary inclusion composite

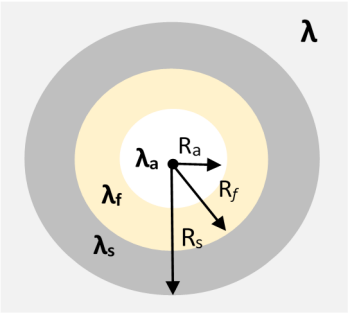


Figure 3 : Double homogenization of auto-coherent model (binder+ vegetable particles)

where a is for air, w is for water and H for hydrated composite

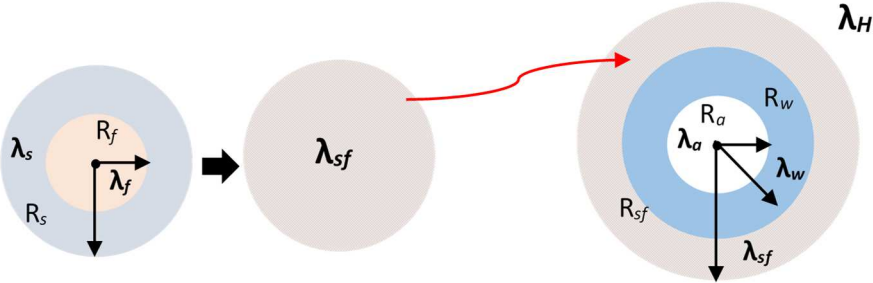


Figure 4 : Bulk density of composites according fiber content in the dry state (RH = 0%)

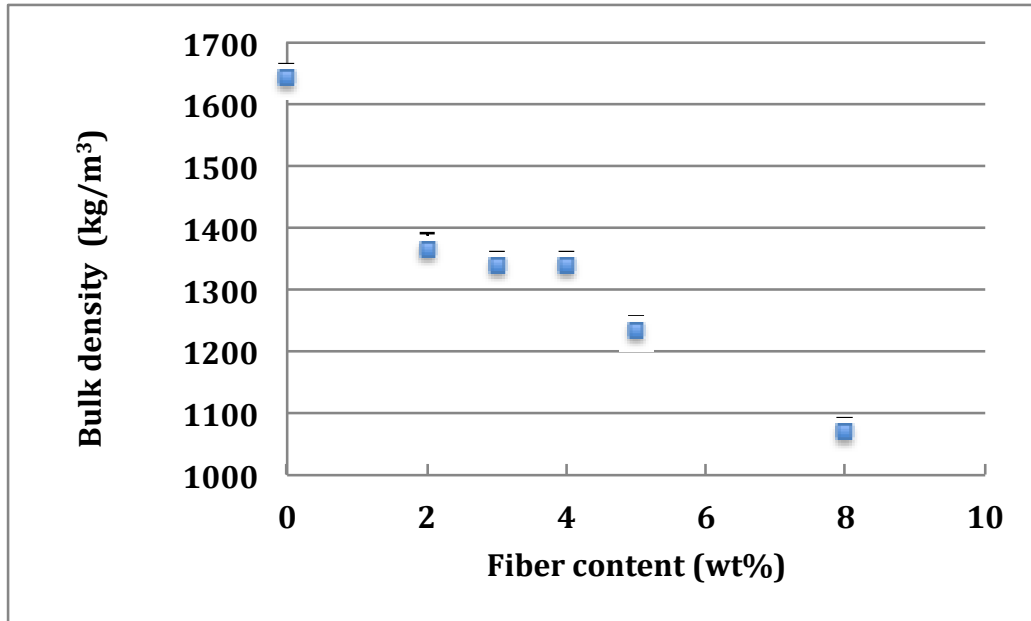


Figure 5 : Porosity of composites according to their fiber content in the dry state (RH = 0%)

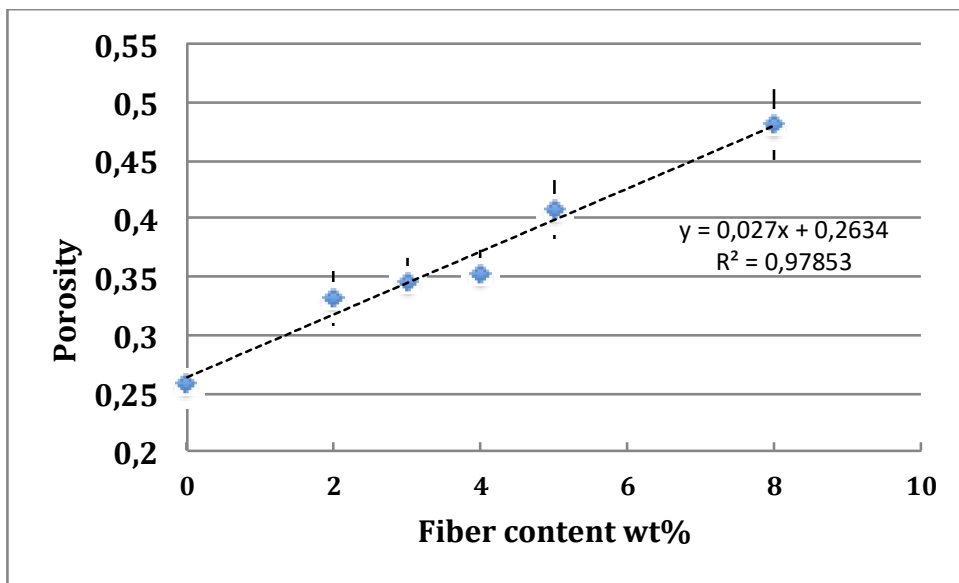


Figure 6 : Thermal conductivity of LFN composites according to fiber content

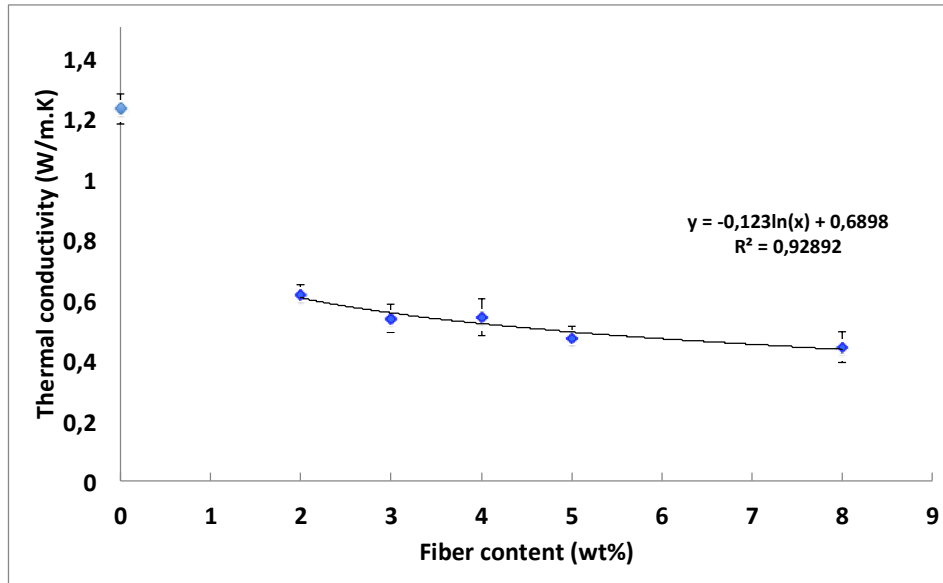


Figure 7: Thermal conductivity of LFN composites according to their bulk density at different moisture contents

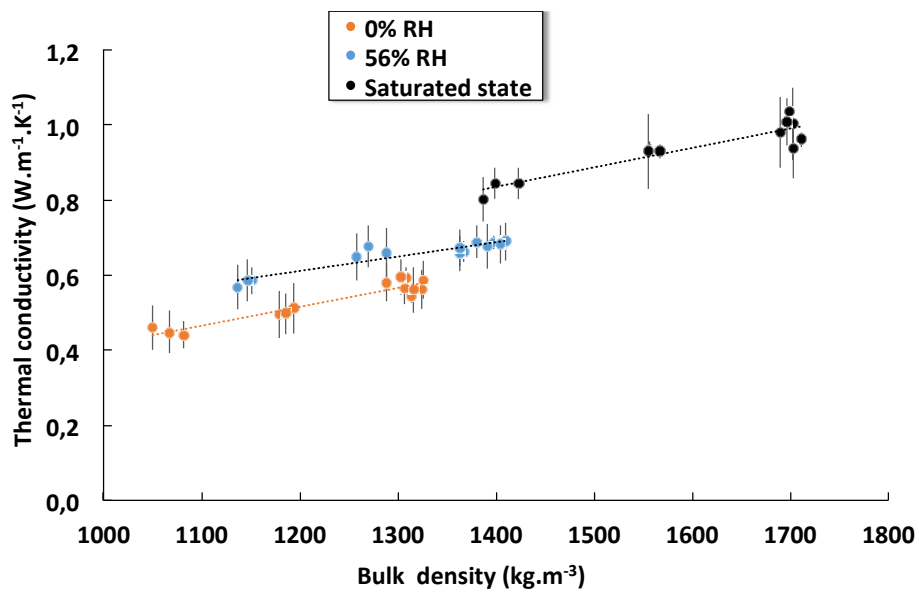


Figure 8: Comparison between theoretical calculations and experimental results of thermal conductivity of dry composites according to bulk density

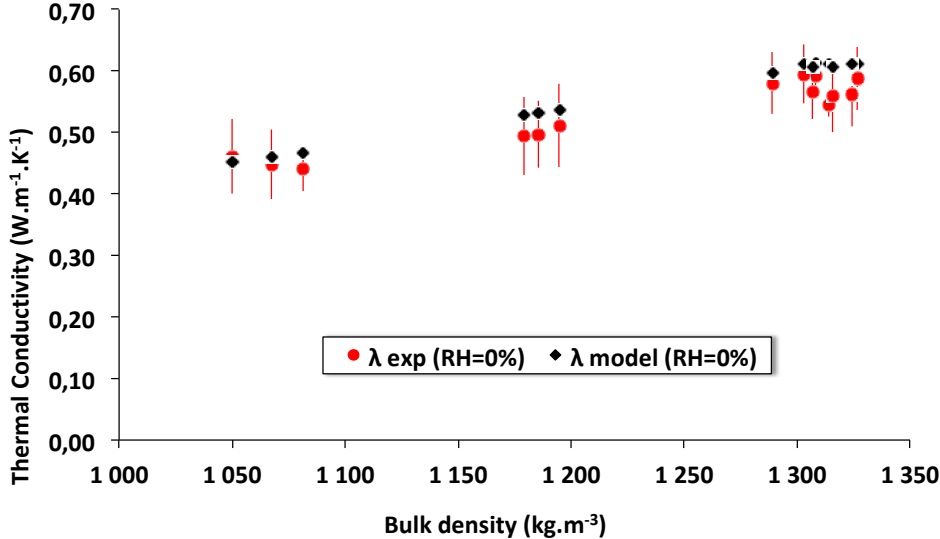


Figure 9: Thermal conductivity varying with bulk density: comparison between theoretical calculations and experimental results (RH=56%)

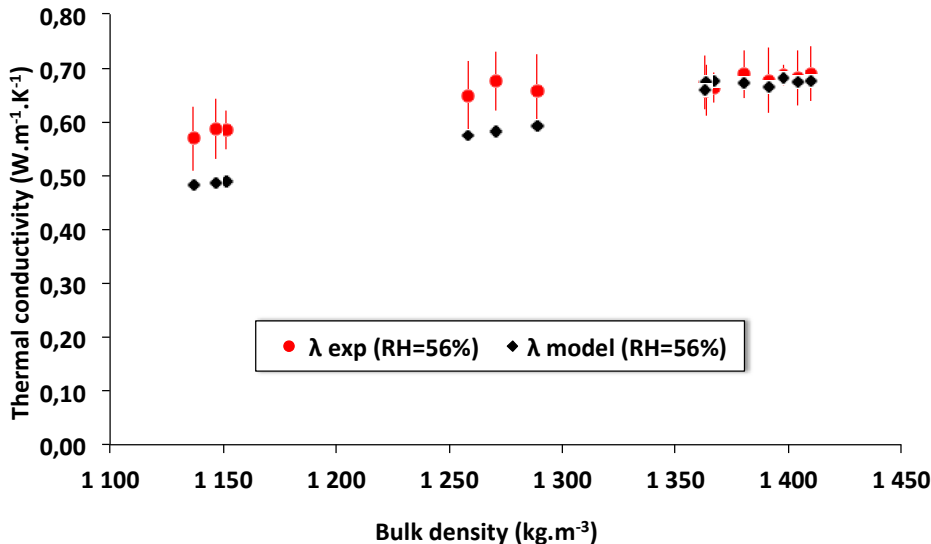


Figure 10: Thermal conductivity varying with bulk density: comparison between theoretical calculations and experimental results (RH=100%)

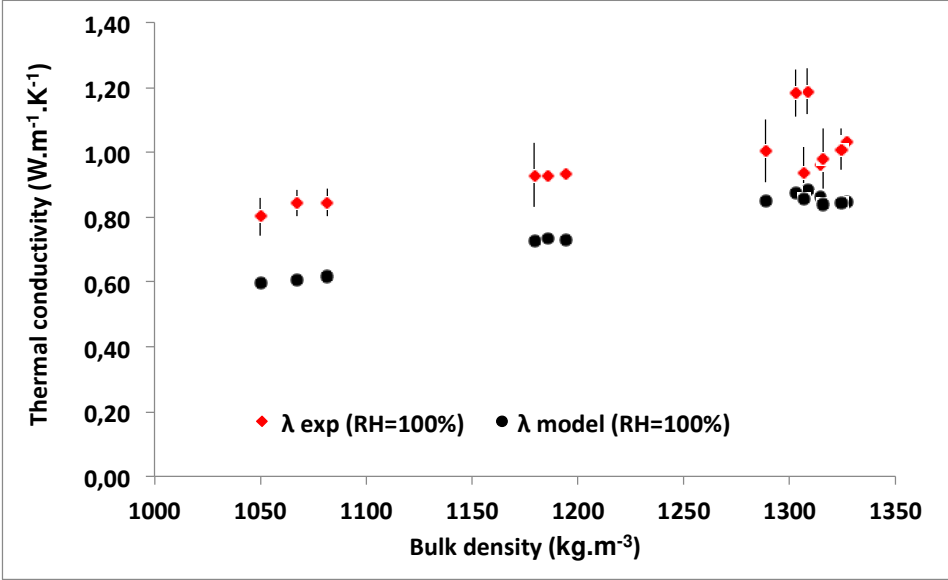


Figure 11 : Sorption isotherms of natural (NBF) and pyrolyzed (TBF) bagasse fibers at (22±3)°C. In red: sorption; in green: desorption.

